JOURNAL OF COMPUTATIONAL PHYSICS 107, 291–296 (1993)

Improved Implicit Residual Smoothing for Steady State Computations of First-Order Hyperbolic Systems

RICKARD ENANDER

Department of Scientific Computing, Uppsala University, Box 120, Uppsala 751 04, Sweden

Received April 21, 1992; revised August 24, 1992

In this paper we introduce a method to accelerate the computation of steady state solutions of first-order hyperbolic problems such as the Euler equations. The acceleration method is an improved version of the so-called *implicit residual smoother*. The new version, the *implicit explicit residual smoother* improves damping properties and numerical examples are presented showing considerably reduction in number of iterations needed to reach a steady state solution.

1. INTRODUCTION

Today CFD, *computational fluid dynamics*, is more and more becoming a design tool in various parts of industrial development, e.g., when designing aircraft or optimizing the drag coefficients of cars. The inviscid flow equations are of hyperbolic type and can be written in conservative form:

$$\frac{\partial}{\partial t} w = \sum_{i=1}^{m} \frac{\partial}{\partial x_i} F_i(w). \tag{1}$$

In Eq. (1) m is the number of space dimensions and F_i are some flux functions. Both time dependent evolutions and stationary solutions are of interest. In this paper we will focus our attention on the cases when a steady state solution is desired. One way to obtain such a solution would be to set the left-hand side of Eq. (1) to zero. The right-hand side should then be discretized in some manner and the system obtained solved. Another commonly used method is to actually integrate the time dependent equation for a long enough time. This is the approach we are going to use in this paper, with an explicit Runge–Kutta method as the time marching method. The problem with explicit time marching methods is that there are stability constraints on the size of the time step that can be used. Typically, for a first-order system, the allowed time step is of the same order as the smallest space step. This restriction makes the computation expensive with respect to CPU time. Since we are not really interested in the time evolution of the solution, we can forget about time accuracy in the iteration and design of the numerical method to accelerate the convergence towards a steady state. The general idea behind all such methods is to increase the *effective time step* that can be used by the underlying scheme in order to propagate waves faster through the computational domain.

Many ways of decreasing the CPU time have been introduced and analyzed, e.g., local time stepping and multigrid methods. In this paper we will analyze the concept of *implicit residual smoothing*, from now on abbreviated IRS, described in [4]. A new smoother, denoted the *implicit explicit residual smoother* and abbreviated the IERS, which considerably improves the convergence properties, will be presented.

2. THE BASIC NUMERICAL METHOD

Let us define the basic numerical method for a test problem in 1D. Consider the first-order system

$$\begin{aligned} v_t &= -v_x, \qquad 0 \leqslant x \leqslant 2\pi, \quad 0 \leqslant t, \\ v(x, 0) &= f(x) \\ v(0, t) &= 1 \end{aligned} \tag{2}$$

which has a steady state solution $v(x, t) = 1$ for $t \geqslant 2\pi$ independent of the initial state $f(x)$. Define a grid $\{x_j = j \cdot h\}$, $j = [0, 1, ..., N]$, on the interval $[0 \leqslant x \leqslant 2\pi]$ with $h = 2\pi/N$ and introduce a grid function $U = \{u_j\}_{j=0}^{N}$ approximating the solution v in Eq. (2). The term v_x is approximated for the grid function U using a second-order accurate finite difference operator,

$$\begin{aligned} \frac{\partial}{\partial x} u_j &\approx \frac{1}{h} (\Delta_0 + \gamma_4 (\Delta_- \Delta_+)^2) u_j \\ \Delta_0 u_j &= \frac{1}{2} (u_{j+1} - u_{j-1}) \\ (\Delta_- \Delta_+)^2 u_j &= u_{j+2} - 4u_{j+1} + 6u_j - 4u_{j-1} + u_{j-2}. \end{aligned} \tag{3}$$

0021-9991/93 $5.00

The parameter γ_4 is chosen to improve damping properties of the scheme for oscillatory modes and is often referred to as the *artifical viscosity coefficient*. The approximation Eq. (3) is used for the grid points $j = [2, 3, ..., N-2]$. In the grid points $j = 1$ and $j = N-1$, where Eq. (3) is not defined, the artificial viscosity term is altered in some way. At the boundary points the following conditions are imposed:

$$\begin{aligned} u_N &= 2u_{N-1} - u_{N-2} \\ u_0 &= 1. \end{aligned} \tag{4}$$

We now have a semidiscrete system

$$\frac{\partial}{\partial t} U = R(U), \tag{5}$$

which is a system of ordinary differential equations with the components in the state vector $U = [u_0, u_1, ..., u_N]$ as unknowns. We will denote the right-hand side of Eq. (5) as the *residual*. In our case an explicit three-stage Runge–Kutta method on the following form is used to integrate Eq. (5) in time

$$\begin{aligned} U^{(0)} &= U^n \\ U^{(1)} &= U^{(0)} + \alpha_1 \cdot \Delta t \cdot R(U^{(0)}) \\ U^{(2)} &= U^{(0)} + \alpha_2 \cdot \Delta t \cdot R(U^{(1)}) \\ U^{(3)} &= U^{(0)} + \alpha_3 \cdot \Delta t \cdot R(U^{(2)}) \\ U^{n+1} &= U^{(3)} \end{aligned} \tag{6}$$

with $\alpha_{1,2,3} = \{0.6,\ 0.6,\ 1.0\}$ resulting in a characteristic polynomial,

$$p(z) = 1 + z + 0.6z^2 + 0.36z^3. \tag{7}$$

The convergence to a steady state this of this scheme depends on wave propagation of smooth parts of the solution and on damping of the oscillatory parts. The strength of the damping is tuned with the parameter γ_4 in Eq. (3). To obtain as effective wave propagation as possible we, of course, want the time step Δt in Eq. (6) to be as large as possible.

To analyze this basic numerical scheme with respect to damping properties and to prepare for the introduction of residual smoothers, we assume periodical boundary conditions and express the solution in Fourier components $[\hat{u}_{-r}, ..., \hat{u}_0, ..., \hat{u}_r]$:

$$u_j = \sum_{\omega=-r}^{r} \hat{u}_\omega e^{i\omega x_j}, \qquad r = N/2. \tag{8}$$

Here ω represents the *wave number* of the Fourier component with $|\omega|$ small meaning smooth components and $|\omega|$ large, oscillatory ones. By inserting Eq. (8) in the spatial discretization Eq. (3) we obtain for every ω an expression for z in the characteristic polynomial Eq. (7),

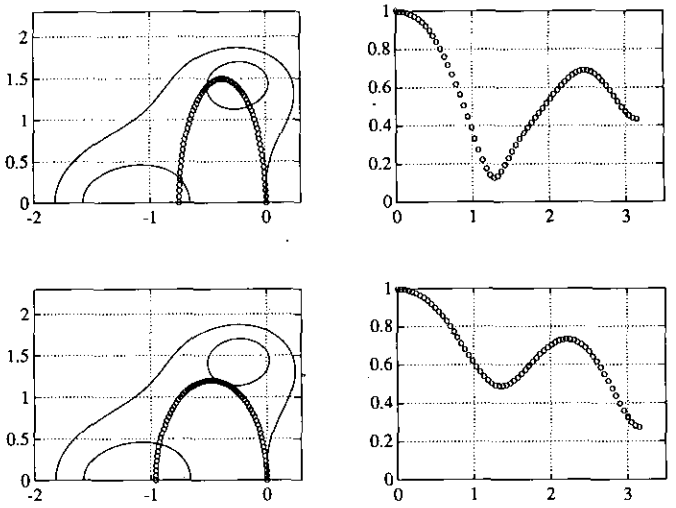

FIG. 1. Fourier symbols and amplification factors.

$$z(\omega) = \lambda \left(i \sin(\omega h) - 16\gamma_4 \sin^4\left(\frac{\omega h}{2}\right)\right), \tag{9}$$

where λ is the ratio between the time step Δt and the spatial step h. To the left in Fig. 1 the Fourier symbol of our spatial discretization is plotted, together with the stability region of the Runge–Kutta scheme. In the figure the two plots at the top are computed with $[\lambda = 1.5,\ \gamma_4 = \frac{1}{32}]$ and the two at the bottom with $[\lambda = 1.2,\ \gamma_4 = \frac{1}{20}]$. Only the part of the symbol with positive imaginary part is plotted since we have symmetry in the real axis. To the right in Fig. 1 we have the amplification factors of the two schemes as a function of $\xi = \omega h$.

3. THE IMPLICIT RESIDUAL SMOOTHER

The general idea with the implicit residual smoother is to increase the time step Δt used in the RK method with a factor α to speed up the wave propagation and thereby reach a steady state in fewer time steps. The scheme will be unstable if α is chosen large, but can be restabilized by applying an implicit smoother to the residual R in Eq. (5). A new smoothed residual $\bar{R}$ is computed as

$$-\beta \bar{R}_{j-1} + (1 + 2\beta)\, \bar{R}_j - \beta \bar{R}_{j+1} = \alpha R_j$$

or

$$(1 - \beta \Delta_- \Delta_+)\, \bar{R}_j = \alpha R_j \tag{10}$$

and the Runge–Kutta time stepping is performed with $\bar{R}$ instead of R. The parameter β determines the strength of the smoothing performed and if β is chosen as

$$\beta = \beta(\alpha) \geqslant \tfrac{1}{4}(\alpha^2 - 1) \tag{11}$$

the scheme can be shown to be stable if the original unsmoothed scheme is stable. This is shown by studying the maximum of the imaginary part of Eq. (13), see [4]. The consequence is that α can be chosen arbitrarily large and thereby the effective time step $\alpha\, \Delta t$ may be arbitrarily large as well. One could now believe that α as large as possible should be the best choice, but in real applications it has been found that α should not be larger than 2–3, see [1–5]. This limitation can be explained in several ways. In Fig. 2 the implicit residual smoother is applied to the model problem for two different α. In the figure it can be seen that the Fourier symbol is contracted to the imaginary axis and this is more accentuated for larger α. This leads to larger amplification factors and poorer damping for $|\omega h|$ large. In real life applications, effective damping for oscillatory modes is crucial since such disturbances are emitted from boundaries and discontinuities in the solution. If these disturbances are not damped out effectively the numerical scheme can converge slower or even become unstable. The Fourier transform of the stencil in Eq. (10) is

$$\mathrm{I\tilde{R}S}(\omega) = \alpha \cdot \frac{1}{1 + 4\beta \sin^2(\omega h/2)} \tag{12}$$

and, together with the Fourier transform of the original stencil Eq. (9), we obtain

$$z(\omega) = \alpha \cdot \frac{1}{1 + 4\beta \sin^2(\omega h/2)} \cdot \lambda \left(i \sin(\omega h) - 16\gamma_4 \sin^4\left(\frac{\omega h}{2}\right)\right) \tag{13}$$

By analyzing Eq. (13) for $\omega h = \pi$ it is easily seen that the symbol is contracted towards the imaginary axis with a factor $\alpha/(1+4\beta)$ or $O(\alpha^{-1})$. Hence, the larger α is, the poorer damping properties we obtain. This effect is more accentuated if problems in two and three space dimensions are considered. In two dimensions we have a $O(\alpha^{-3})$ contraction and in three dimensions, $O(\alpha^{-5})$.

4. A NEW RESIDUAL SMOOTHER

To overcome the deteriorated damping of highly oscillatory modes for large α in Eq. (10) we propose a new version of the residual smoother. Compute the smoothed residual $\tilde{R}$ as

$$(1 - \beta \Delta_- \Delta_+)\, \tilde{R}_j = \alpha (1 - \gamma \Delta_- \Delta_+)\, R_j. \tag{14}$$

The difference compared to the I-smoother, Eq. (10), is the operator $(1 - \gamma \Delta_- \Delta_+)$ on the explicit side and from now on we will refer to this version as the *implicit–explicit residual smoother* or the IERS. The Fourier transform of this smoothing operator is

$$\mathrm{IE\tilde{R}S}(\omega) = \alpha \cdot \frac{1 + 4\gamma \sin^2(\omega h/2)}{1 + 4\beta \sin^2(\omega h/2)} \tag{15}$$

and, combining this with Eq. (9), we obtain for the total spatial discretization

$$z(\omega) = \alpha \cdot \frac{1 + 4\gamma \sin^2(\omega h/2)}{1 + 4\beta \sin^2(\omega h/2)} \cdot \lambda \left(i \sin(\omega h) - 16\gamma_4 \sin^4\left(\frac{\omega h}{2}\right)\right) \tag{16}$$

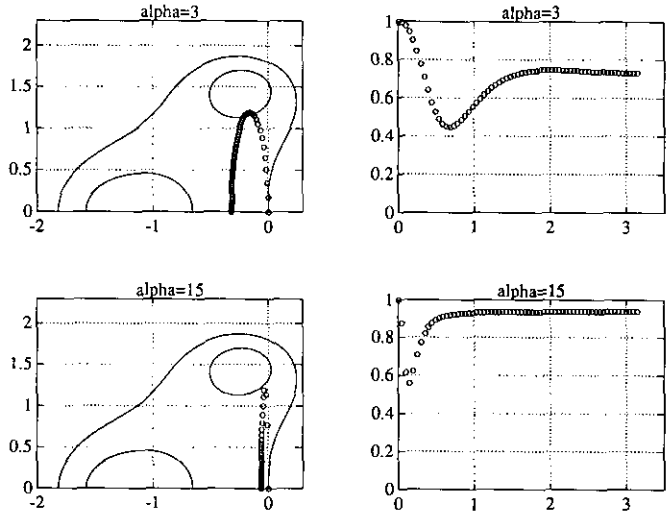

FIG. 2. Model problem with IRS.

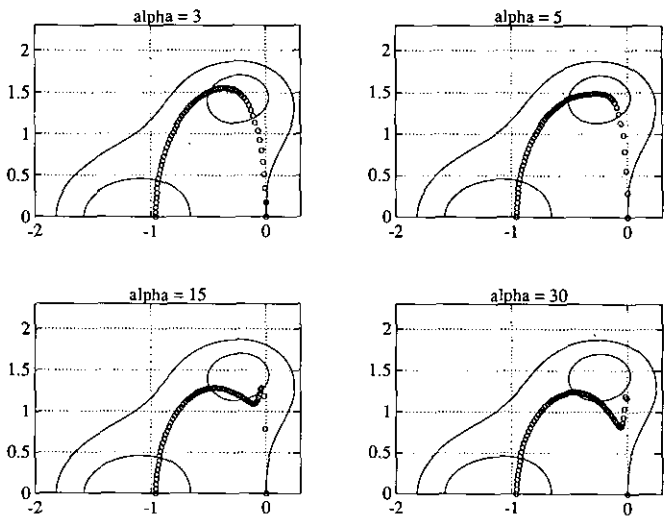

FIG. 3. Model problem with IERS.

By inserting $\omega h = \pi$ in Eq. (16) and demanding the same damping properties as in Eq. (9) we obtain the condition for the parameter γ,

$$\gamma = \gamma(\alpha) = \frac{1}{4}\left(\frac{1+4\beta}{\alpha} - 1\right) \tag{17}$$

In Fig. 3 four different cases of Fourier symbols for the IERS are plotted for different values of α. It should be noted that for $|\omega h| \approx \pi$, the spectra have more or less identical behavior with a real part of $-16\lambda\gamma_4$. With larger α the spectral points for $|\omega h|$ small are pushed away from origin, indicating an increasing effective time step. One minor problem for the IERS with small α can also be detected in Fig. 3: The maximum of the imaginary part of the symbol is larger than for the original scheme. We therefore have a potential risk for the scheme to become unstable.

In Fig. 4 the overshoot is plotted as a function of α. The overshoot is very moderate and decreases for larger α and, since we are really interested in having large α, this is not a crucial problem. One way of guaranteeing the Fourier symbols remain inside the stability domain of the Runge–Kutta scheme is to divide the parameter λ by the number obtained in Fig. 4. If, for example, we would like to use $\alpha = 10$, λ should be divided by ≈ 1.1 and the effective time step would then be $10/1.1 \approx 9$ times larger than for the original scheme.

In Fig. 3 we can also see that for large α the Fourier symbol has a local minimum and that this minimum is smaller for α larger. In Fig. 5 the imaginary part of the Fourier symbol is plotted as a function of $\xi = \omega h$ for four different α. A more careful analysis of these extrema is carried out in [2, p. B.22–24] and it is found that:

(a) A maximum $O(1)$ for $\xi_{\max} = O(\alpha^{-1})$

(b) A minimum $O(\alpha^{-1/2})$ for $\xi_{\min} = O(\alpha^{-1/2})$.

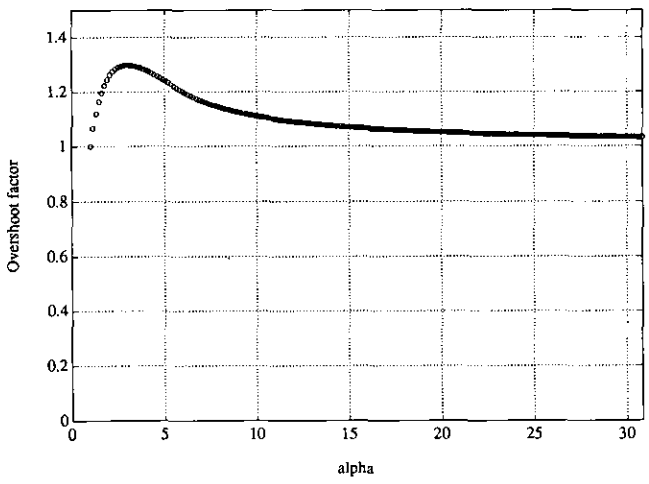

FIG. 4. Overshoot of IERS as function of effective time step.

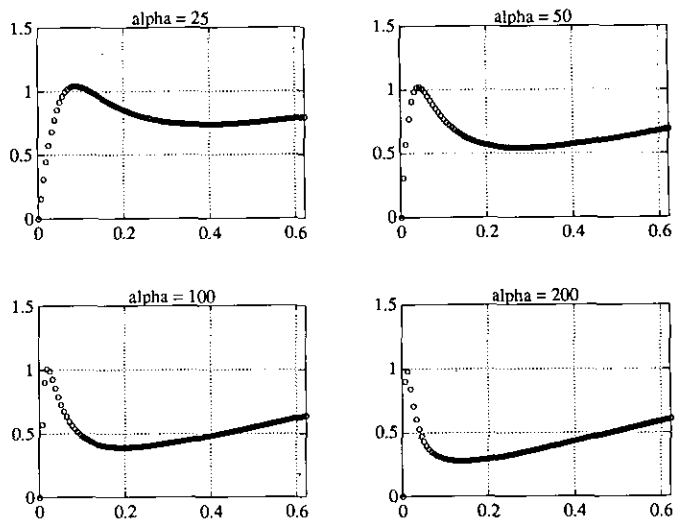

FIG. 5. Imaginary part for large effective time step.

These extrema indicate a upper limit for the choice of α which should not be larger than a value $\bar{\alpha}$ for which the imaginary part of the Fourier spectrum is equal for $\xi = h$ and the minimum. A larger α forces the minimum to be smaller than the first spectral point h. The upper limit for α is then a function of the spatial step h and a smaller h leads to a larger upper limit $\bar{\alpha}$. In Fig. 5 we can see that this upper limit $\bar{\alpha}$ lies somewhere between 50 and 100 for this particular choice of spatial step h.

5. NUMERICAL EXAMPLES

Let us start with our model problem equation (1) and integrate from some random initial state to a steady state. With a steady state we mean that the L_2-norm of the time derivative of the solution is below 10^{-6}.

In Table I the number of iterations needed to compute the steady state is listed for different numbers of grid points N for the plain Runge–Kutta iteration and for the two smoothed versions. For the two residual smoothers the best choice of the parameter α is listed in the table. From the

TABLE I

Model Problem

	Plain RK	RK + IRS		RK + IERS	
N	No. iter.	No. iter.	Best α	No. iter.	Best α
64	104	64	2	34	8
128	174	91	3	41	11
256	306	123	4	50	14
512	571	171	5	66	17
1024	1088	250	6	87	22
2048	2119	364	8	118	29

table it is clear that the required number of iterations is considerably reduced when using the two smoothers with the IERS as the best choice. It can also be noted that the relative speedup of the IERS increases with the number of grid points and that the optimal α also is larger for the IERS.

We now consider the quasi-one-dimensional Euler equations for flow in a converging–diverging channel. The equations are written in the form

$$\frac{\partial q}{\partial t}+\frac{\partial F}{\partial x}=g, \qquad -1\leqslant x\leqslant 1$$

$$q=\begin{pmatrix}\rho A\\ \rho uA\\ E_sA\end{pmatrix}, \quad F=\begin{pmatrix}\rho uA\\ (\rho u^2+p)A\\ u(E_s+p)A\end{pmatrix}, \quad g=\begin{pmatrix}0\\ p\frac{dA}{dx}\\ 0\end{pmatrix}$$

$$E_s=\frac{p}{\gamma-1}+\frac{\rho}{2}u^2, \tag{18}$$

where $\gamma=c_p/c_v$ is the ratio between the heat capacities at constant pressure c_p and constant volume c_v. A is the channel area given by

$$A(x)=1+\tfrac{1}{2}(1-\cos(\pi x)), \qquad -1\leqslant x\leqslant 1.$$

We use boundary data so that the computed steady state solution contains a shock. The same Runge–Kutta smoother is used as for the model problem above with the difference that, in addition to the fourth-order artificial viscosity, we now also have a second-order term in such a way that Eq. (3) is altered to

$$\frac{\partial}{\partial x}u_j\approx\frac{1}{h}(\Delta_0+\gamma_4(\Delta_-\Delta_+)^2-\gamma_2(\Delta_-\Delta_+))\,u_j. \tag{19}$$

The parameter γ_2 is for a given grid point j computed as

$$\gamma_2=\kappa_2\cdot\frac{|p_{j-1}-2p_j+p_{j+1}|}{|p_{j-1}+2p_j+p_{j+1}|}.$$

This second-order dissipation is added with the purpose of preventing unphysical oscillations near shocks. For more details see, for example, [4]. In Table II we have the same comparison between the methods as in Table I. The same pattern can be noted, a considerable reduction in the required number of iterations and the IERS as the best choice, but the improvement is not as striking as in the scalar case.

6. MULTIGRID ITERATION

Before talking about the multigrid method something about the meaning of the word *smoother* must be said. On one hand, we have a Runge–Kutta iteration method with or without *residual smoother* and, on the other hand, will this Runge–Kutta iteration be used as a *smoothing operator* in the multigrid cycle. Hopefully the meaning of the word smoother will be clear from the context in which it is used. Multigrid iteration is another commonly used method of increasing the convergence rate. The scheme described so far is then used as the smoothing operator. The multigrid method is more complicated to analyze with the Fourier transform, since restriction and prolongation operators between different grid levels couple the Fourier modes together. See, for example [3], how this coupling affects the damping properties. One rule of thumb when designing a smoothing operator in a multigrid cycle is that the damping for highly oscillatory modes shall be effective. We can therefore expect the IERS to be a better choice than the IRS in such a situation.

In Tables III and IV we have a simple multigrid case with two grid levels. The most striking difference when comparing Table III to table I is that the optimal choice of α for the IRS is so much lower in the multigrid case, which is in line with the rule of thumb mentioned above.

For the Euler case in Table IV the difference between the IERS and the IRS is less striking than in the scalar case, but the gain is, about 40%.

TABLE II

Quasi-1D Euler Case

	Plain RK	RK + IRS		RK + IERS	
N	No. iter.	No. iter.	Best α	No. iter.	Best α
64	866	622	1.6	430	2.4
128	1746	1235	1.6	869	3.8
256	3427	1570	2.4	1106	5.0
512	7228	2469	3.2	1706	6.6
1024	13640	4047	3.8	2491	8.0

TABLE III

Model Problem, Multigrid with Two Grid Levels

	Plain RK	RK + IRS		RK + IERS	
N	No. iter.	No. iter.	Best α	No. iter.	Best α
64	46	45	1.7	27	8
128	67	54	1.8	28	7
256	114	74	2.1	30	10
512	205	107	2.4	33	16
1024	377	165	2.6	40	23
2048	724	280	2.8	51	28

TABLE IV

Quasi-1D Euler Case, Multigrid with Two Grid Levels

	Plain RK	RK + IRS		RK + IERS	
N	No. iter.	No. iter.	Best α	No. iter.	Best α
128	636	524	1.4	384	2.8
256	1219	895	1.6	603	3.4
512	2435	1445	1.8	929	4.0
1024	5003	2107	3.0	1285	5.0

7. CONCLUSIONS AND REMARKS

In this paper we have proposed the IERS, a new improved version of the IRS. The IERS possesses much better damping properties than the IRS when analyzed with the Fourier transform, which indicates that a larger effective time step $\alpha\,\Delta t$ could be used in real life applications. This is also shown with numerical examples both for single grid iterations and for multigrid cycles. Since damping properties deteriorate more in several space dimensions for the IRS, the IERS would be a promising candidate for convergence acceleration when it is generalized to 2D and 3D. This can be done in a relatively straightforward manner.

One remark about number of iterations versus the actual CPU time: In this paper the number of iterations are presented for the examples rather than the CPU time. The extra cost for the IRS in 1D is to solve a three-diagonal system in each Runge–Kutta stage for each state variable in the system. For the IERS there is an additional evaluation of an explicit three-point stencil. This computational overhead is less significant if the equation itself and the numerical scheme are complicated than for the simple scalar case. In the quasi-1D case the overhead is approximately 15% for the IRS and 30% for the IERS, compared to the unsmoothed iteration.

Finally, a remark about the choice of the time stepping. There are a large variety of Runge–Kutta schemes in use for the numerical method described in this paper. Two to five stages are used and sometime the artificial viscosity are not evaluated in all stages. The important property of the IERS is the non-contracting Fourier symbol which is important for all choices of Runge–Kutta time stepping.

REFERENCES

1. R. V. Chima, E. Turkel, and S. Schaffer, NASA Technical Memorandum 88878, ICOMP-86-3, 1986.
2. R. Enander, Doctorial thesis, Uppsala University, Department of Scientific Computing, 1991 (unpublished).
3. B. Gustafsson and P. Lötstedt, in *Proceedings, Fourth Copper Mountain Conf. on Multigrid Methods, 1989* (SIAM, Philadelphia, 1989), p. 181.
4. A. Jameson, *Comm. Pure Appl. Math.* **41**, 507 (1988).
5. E. Turkel, ICASE Report No. 84-32.